# Mutations in the murine erythroid α-spectrin gene alter spectrin mRNA and protein levels and spectrin incorporation into the red blood cell membrane skeleton

Nancy J. Wandersee, Connie S. Birkenmeier, David M. Bodine, Narla Mohandas, and Jane E. Barker

Tetramers of α- and β-spectrin heterodimers, linked by intermediary proteins to transmembrane proteins, stabilize the red blood cell cytoskeleton. Deficiencies of either α- or β-spectrin can result in severe hereditary spherocytosis (HS) or hereditary elliptocytosis (HE) in mice and humans. Four mouse mutations, *sph*, *sph^Dem^*, *sph^2BC^*, and *sph^J^*, affect the erythroid α-spectrin gene, *Spna1*, on chromosome 1 and cause severe HS and HE. Here we describe the molecular alterations in α-spectrin and their consequences in *sph^2BC^/sph^2BC^* and *sph^J^/sph^J^* erythrocytes. A splicing mutation, *sph^2BC^* initiates the skipping of exon 41 and premature protein termination before the site required for dimerization of α-spectrin with β-spectrin. A nonsense mutation in exon 52, *sph^J^* eliminates the COOH-terminal 13 amino acids. Both defects result in instability of the red cell membrane and loss of membrane surface area. In *sph^2BC^/sph^2BC^*, barely perceptible levels of messenger RNA and consequent decreased synthesis of α-spectrin protein are primarily responsible for the resultant hemolysis. By contrast, *sph^J^/sph^J^* mice synthesize the truncated α-spectrin in which the 13-terminal amino acids are deleted at higher levels than normal, but they cannot retain this mutant protein in the cytoskeleton. The *sph^J^* deletion is near the 4.1/actin-binding region at the junctional complex providing new evidence that this 13-amino acid segment at the COOH-terminus of α-spectrin is crucial to the stability of the junctional complex. (Blood. 2003;101:325-330)

© 2003 by The American Society of Hematology

## Introduction

Mice with mutations in genes encoding membrane skeletal proteins are important models for hereditary spherocytosis (HS).[1] Gene mapping and disrupted protein levels[2,3] identified the affected product and became the basis for the subsequent cloning and sequencing of α-spectrin *(Spna1)*, β-spectrin *(Spnb1)*, and ankyrin *(Ank1)* from mouse[4-6] and human DNA.[7-10] β-Spectrin is a pivotal protein that provides binding sites for ankyrin, the linker between spectrin and the transmembrane protein band 3; α-spectrin heterodimerization; tetramerization of heterodimers[11]; and 4.1, a protein that joins spectrin tetramers to the transmembrane protein glycophorin C at junctional complexes.[12] Anchoring of the spectrin-based cytoskeleton to the transmembrane proteins band 3 and glycophorin C is essential for red blood cell stability. The nucleotide alterations described for the mouse beta spectrin *(ja/ja)*,[13] ankyrin *(nb/nb)*,[14] and α-spectrin *(sph/sph, sph^Dem^/sph^Dem^)*[4,15] mutations provide an explanation for the instability of red cells in these mutants and clues to the functional consequences of alterations in specific amino acids. Assessing functional effects of mutations in humans is more difficult because the secondary genetic diversity affects results, mutations are heterogeneous, and clinical severity may vary among patients with the same mutation.

The murine α-spectrin mutations *sph*, *sph^2BC^*, and *sph^J^* result in severe HS, whereas *sph^Dem^* is a unique model for hereditary elliptocytosis (HE).[16] α-Spectrin–deficient mice, such as *ja/ja* and *nb/nb*, have severe anemia, reticulocytosis, splenomegaly, hepato-megaly, and cardiomegaly.[1] Mice with a complete lack of α-spectrin, unlike those with no β-spectrin,[17] can live to adulthood,[18] indicating a less critical role for α-spectrin than β-spectrin. The frequency of thrombosis and stroke, recently described consequences of murine severe hemolytic anemia, is higher (85%-100%) in α-spectrin–deficient mice than in either *nb/nb* (15%) or neonatally transfused *ja/ja* mice.[19-21]

As originally predicted, identification of the mutated site for each allele provides insight into the functional effects of regional alterations or complete ablation of specific cytoskeleton proteins. Murine mutations are maintained on the same genetic background, precluding any effects of modifier genes on their function. Elucidation of primary and secondary effects of the mutations can be performed in vitro and in vivo. The molecular defect in the *sph* allele is a single-base deletion in exon 11 of *Spna1* that causes a frame-shift, a premature termination of α-spectrin mRNA, and an absence of protein.[4] In *sph^Dem^*, an intracisternal A particle element is inserted in intron 10 of the *Spna1* gene; exon 11 is skipped with the in-frame deletion of 46 amino acids from the α-spectrin protein.[16]

Preparatory to further analyses at the cellular level, we have identified the molecular defects in the remaining 2 mutant α-spectrin HS alleles, *sph^2BC^* and *sph^J^*, and have characterized functional differences in their red blood cells. The *sph^2BC^/sph^2BC^* mice generate barely detectable levels of a truncated α-spectrin that

lacks the β-spectrin dimerization site. Reticulocytes from $sph^J/sph^J$, when compared to $+/+$, translate higher levels of a truncated α-spectrin lacking the 13 COOH-terminal amino acids. This protein, however, is not stably maintained in the membrane cytoskeleton. This finding enables us to identify a previously unsuspected functional role for this region of α-spectrin in cytoskeletal stabilization, possibly through the regulation of interactions between the spectrin tetramer and junctional complex proteins.

## Materials and methods

### Animals

Mice heterozygous for the $sph^{2BC}$ and $sph^J$ mutations were maintained congenic on both WB/Re (WB) and C57BL/6J (B6) backgrounds. F1 hybrid (WBB6F1) $sph^{2BC}/sph^{2BC}$ and $sph^J/sph^J$ mice and their normal $sph^{2BC}/+$, $sph^J/+$, and $+/+$ littermates were generated by mating heterozygous WB and B6 mice. Mice were housed and cared for according to Association for Assessment and Accreditation of Laboratory Animal Care (AAALAC) specifications.

### RT-PCR and sequencing of α-spectrin

Normal phenylhydrazine-treated[22] and mutant mice were transcardially perfused with cold 1× phosphate-buffered saline (PBS; Gibco/BRL, Grand Island, NY). Total RNA from spleens was isolated using Trizol reagent (Gibco/BRL). Reverse transcription–polymerase chain reaction (RT-PCR) was performed as previously described on total spleen RNA from $+/+$, $sph^{2BC}/sph^{2BC}$, and $sph^J/sph^J$ mice.[4,16] Fragments were sequenced by the dideoxynucleotide chain termination method[23] using M13 forward and reverse primers and T7 DNA polymerase (TaqFS; ABI, Foster City, CA). Sequence data were analyzed using the Sequencher DNA analysis software package (ABI).

### Genomic PCR and sequencing

Isolation and PCR of genomic spleen DNA from $+/+$, $sph^{2BC}/+$, and $sph^{2BC}/sph^{2BC}$ mice were performed as previously described.[4,16] Genomic PCR products were sequenced and analyzed as described above. Tail DNA PCR was performed in 2 reactions on genomic DNA from $+/+$, $sph^{2BC}/+$, and $sph^J/+$ mice, as described by the manufacturer.[24] For the $sph^{2BC}$ mutation, a common downstream primer was used (primer 54, 5′-GTC-CTGTGGGTTTATGCCA-3′). Upstream primers detected either only the $sph^{2BC}$ allele (primer 52, 5′-TAGTGGAATCCTGGGATAGT-3′) or the wild-type and the $sph^{2BC}$ alleles (primer 53, 5′-GTAGTGGAATCCTG-GATAG-3′) of $Spna1$. For $sph^J$, the upstream primer was common (primer 47, 5′-CTCTCACCCCGGAACAA-3′). Downstream primers detected either only the $sph^J$ allele (primer 49, 5′-GTGAAGCCAACATAGTCT-3′) or both the wild-type and the $sph^J$ alleles (primer 50, 5′-TGGTGAAGCCAA-CATAGTC-3′) of $Spna1$. PCR products were electrophoresed on 2% SeaPlaque-GTG (FMC, Rockland, ME) agarose gels.

### Northern blot analyses

Total RNA was extracted from reticulocytes, and spleens were retrieved from normal phenylhydrazine-treated and mutant mice as described above. Northern blot analyses on 5 μg total RNA were performed using the NorthernMax kit and BrightStar Plus membranes (Ambion, Austin, TX). Equivalency of RNA loading was verified by UV shadowing.[25] Antisense RNA probe corresponding to nucleotides 7065 to 7322 of the murine erythroid α-spectrin cDNA sequence (GenBank accession no. AF093576) was produced and $^{32}$P-labeled using the Lig'n'Scribe and StripEZ labeling kits and SP6 RNA polymerase (Ambion). Filters were hybridized at 65°C in NorthernMax hybridization buffer (Ambion). Final filter wash was at 65°C in 0.1 × SSC (sodium chloride/sodium citrate), 0.1% sodium dodecyl sulfate (SDS).

### SDS-PAGE and immunoblot analyses

Red blood cell (RBC) ghosts were prepared from packed red blood cells as previously described.[2] Equal amounts of ghost proteins were electrophoresed on 4% stacking/10% separating Laemmli sodium dodecyl sulfate–polyacrylamide gel electrophoresis (SDS-PAGE) gels[26] or on nongradient gels.[27] Duplicate gels were run; one was stained with Coomassie brilliant blue and the other transferred to Immobilon-P membranes (Millipore, Bedford, MA).[28] Band intensities in Coomassie blue–stained gels were quantified using a Molecular Dynamics Densitometer and ImageQuant software (Molecular Dynamics, Sunnyvale, CA). Immunostaining was performed using the Alkaline Phosphatase Conjugate Substrate Kit (Bio-Rad, Hercules, CA). Immunoblots were probed with a rabbit polyclonal antibody to purified mouse erythroid spectrin that reacts equivalently to α- and β-spectrin.[2]

### Osmotic gradient ektacytometry

Fresh blood samples were continuously mixed with a 4% polyvinylpyrrolidone solution of gradually increasing osmolality (60-600 mOsm). The deformability index was recorded as a function of osmolality at a constant applied shear stress of 170 dyne/cm$^2$ using an ektacytometer (Bayer Diagnostics, Tarrytown, NY).[29]

### α-Spectrin incorporation into erythrocyte ghosts

Reticulocyte-rich blood was collected in hematocrit tubes from the intraorbital sinus of $sph^J/sph^J$ and phenylhydrazine-treated $+/+$ mice. The tubes were centrifuged in an Autocrit II (Fisher Scientific), and the white blood cell and plasma layers were discarded. Aliquots of $1 \times 10^8$ reticulocytes were incubated in 300 μL NCTC-109 (MA Bioproducts, Boston, MA) with 10% fetal calf serum (MA Bioproducts) at 37.5°C in 5% $CO_2$ in air. Cells were labeled by incubation with 50 μCi [$^{35}$S] methionine or [$^3$H] leucine. Labeled amino acids were chased with 5 mg appropriate cold amino acid. Methionine and leucine were chosen because of the availability of high specific activity preparations and because α-spectrin contains equal molar percentages of each. Under the culture conditions used, incorporation of radiolabel into α-spectrin is continuous in normal and $sph^J/sph^J$ reticulocytes for 70 minutes. Aliquots of cells were removed at various time points during labeling and cold chase. Whole-cell lysates were assayed by immunoprecipitation.[30] Ghost proteins were separated on 3.5% Fairbanks SDS-PAGE gels.[27] The α-spectrin band was cut from the dried gels and solubilized in NCS tissue solubilizer (Amersham, Piscataway, NJ) and Omnifluor (NEN, Boston, MA),[31] and the amount of [$^{35}$S]- and [$^3$H]-labeled α-spectrin was determined by scintillation counting in a Beckman spectrometer.

## Results

### Identification of the $sph^{2BC}$ mutation

RT-PCR was used to identify the α-spectrin mutation in total RNA from $sph^{2BC}/sph^{2BC}$ spleen. Comparison of cDNA sequence from $+/+$ and $sph^{2BC}/sph^{2BC}$ mice indicated that exon 41 was absent in the α-spectrin mRNA of the latter (Figure 1A). This 162-nucleotide (nt) deletion removes 54 amino acids (aa) from the α-spectrin protein, resulting in a frame-shift and subsequent premature protein termination. No other anomalies were found in the mutant α-spectrin cDNA sequence.
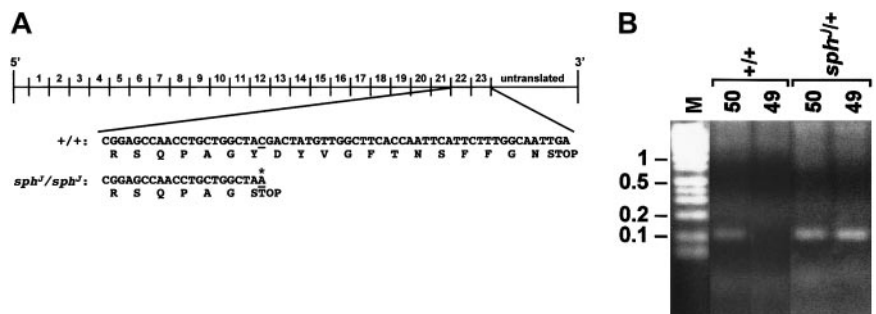
Amplification of genomic spleen DNA using exon 41–specific primers showed that exon 41 is present in $sph^{2BC}/sph^{2BC}$ mice (data not shown). This suggested a mutation within exon 41 or within flanking introns causes aberrant splicing and the skipping of exon 41 in the mature mRNA. Sequencing of exon 41 and intron 40 from genomic DNA revealed no discrepancies between normal and mutant sequences (data not shown). Sequencing of intron 41 revealed a G-to-T transition in the first
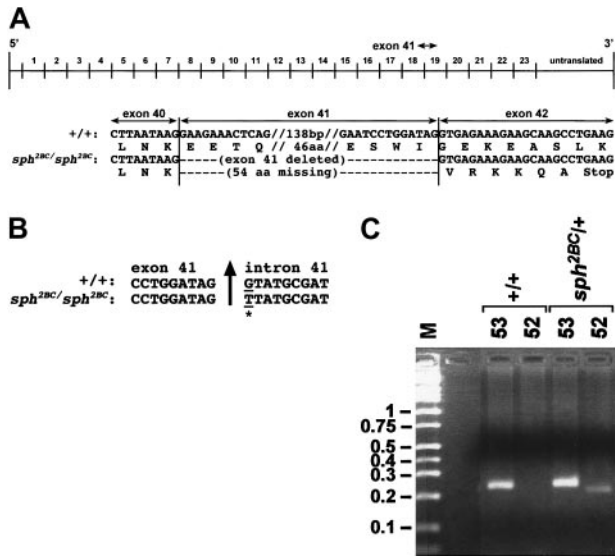
**Figure 1. Mutation in sph²ᴮᶜ.** (A) Top, schematic representation of the *Spna1* cDNA with numbers above the line corresponding to the repeats of 106 aa that comprise the α-spectrin protein. Exon numbering infers correspondence to the human. Arrow above the line shows the location of exon 41. Shown below the cDNA schematic is nucleotide (top) and amino acid (bottom) sequence of the +/+ and *sph²ᴮᶜ/sph²ᴮᶜ* cDNAs in the vicinity of the exon 41 skip. Double hatch marks (//) denote sequences not represented in the figure; numbers of base pairs (bp) and amino acids (aa) not represented are shown between the hatch marks. (B) α-Spectrin genomic sequence at the exon 41/intron 41 boundary obtained from spleen DNA of wild-type (+/+) and *sph²ᴮᶜ/sph²ᴮᶜ* mice. Upward arrow denotes exon 41/intron 41 boundary. The mutated base in the *sph²ᴮᶜ* allele is marked by an underline and an asterisk. (C) Representative genomic PCR of tail DNA from +/+ and *sph²ᴮᶜ/+* mice. Lane M is marker; sizes in kb are shown on left. Lanes labeled 53: PCR products from a reaction containing primers (53 and 54) that amplify wild-type and mutant alleles of *Spna1*. Lanes labeled 52: PCR products from a reaction containing primers (52 and 54) designed to identify the G→T transition in the *sph²ᴮᶜ* allele. Genotype of mice is noted above each bracketed pair of reactions.

base of intron 41 in the *sph²ᴮᶜ* allele of *Spna1* (Figure 1B). To confirm that this sequence anomaly is the *sph²ᴮᶜ* mutation, genomic PCR of tail DNA from +/+ and *sph²ᴮᶜ/+* mice was performed. PCR with primers designed to identify normal and mutant α-spectrin alleles yields a product in +/+ and *sph²ᴮᶜ/+* mice (lanes labeled 53, Figure 1C). Amplification with primers that identify the G-to-T transition is successful only in *sph²ᴮᶜ/+* mice (lanes labeled 52, Figure 1C). The size difference between the mutant (52) product and the control (53) product is owing to a difference in the length of a CA repeat in intron 41 between the wild-type and the *sph²ᴮᶜ* alleles of *Spna1*. Further PCR analyses demonstrated a decreased CA repeat length in the *sphᴶ* and wild-type C3HeBFeJ alleles of *Spna1*, the stock on which *sph²ᴮᶜ* originated. This confirms that a change in CA repeat length is a polymorphism and not the actual mutation. No other alterations were detected. We concluded that the G-to-T transition is the *sph²ᴮᶜ* mutation.

### Identification of the *sphᴶ* mutation

Identification of the *sphᴶ* mutation was performed in a similar manner. Analyses of cDNA sequences from +/+ and *sphᴶ/sphᴶ* mice identified a C-to-A transition in exon 52 of the *sphᴶ/sphᴶ* cDNA (Figure 2A). This nonsense mutation converts a tyrosine to a stop codon, eliminating the COOH-terminal 13 aa from the protein.
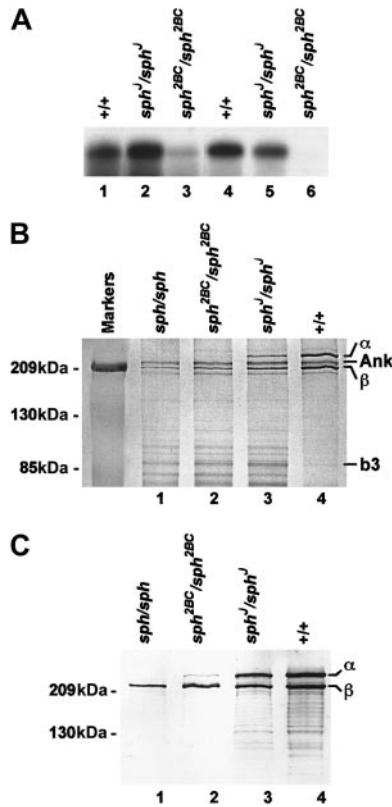
The identity of the *sphᴶ* mutation was confirmed through genomic PCR of tail DNA from known +/+ and *sphᴶ/+* mice. PCR with primers designed to identify normal and mutant α-spectrin alleles yields a product in +/+ and *sphᴶ/+* mice (lane labeled 50, Figure 2B). Amplification with primers designed to identify the C-to-A transition is successful only in *sphᴶ/+* mice (lanes labeled 49, Figure 2B). These data confirm that the C-to-A transition segregates with the *sphᴶ* mutation. The 13 aa deleted as the result of the *sphᴶ* mutation include neither the dimerization site nor the EF hands of α-spectrin. Nevertheless, it is clear from the extreme reticulocytosis and dramatically reduced red cell counts[18] that these 13 aa constitute an important functional domain and are critical to stabilize the cytoskeleton.

### Effect of the mutations on RNA and protein levels

Previously, we showed that erythroid α-spectrin transcript levels in *sph²ᴮᶜ/sph²ᴮᶜ* spleen, the major site of red blood cell production in the mouse, and reticulocytes are decreased compared with +/+.[2] Here we show that the deficiency of *sph²ᴮᶜ/sph²ᴮᶜ* α-spectrin mRNA is more pronounced in reticulocytes than spleen (Figure 3A), suggesting that the mutant form is unstable and degraded as erythroid precursors mature. By contrast, the erythroid α-spectrin mRNA levels are higher than normal in *sphᴶ/sphᴶ* spleens, though they, too, decrease during maturation. At steady state, α-spectrin in *sph²ᴮᶜ/sph²ᴮᶜ* is not detectable on SDS-PAGE gels of reticulocyte ghosts by Coomassie blue staining, but it is reduced to 20% of normal in *sphᴶ/sphᴶ* (Figure 3B). Other cytoskeletal proteins are deficient as well: α-spectrin–band 3 ratios of 0% and 7.7% of normal, β-spectrin–band 3 ratios of 8% and 14% of normal, and ankyrin–band 3 ratios of 20% and 25% of normal in *sph²ᴮᶜ/sph²ᴮᶜ* and *sphᴶ/sphᴶ*, respectively (Table 1). Immunoblot analyses of RBC ghosts with an antibody that reacts similarly to α- and β-spectrin confirm that α-spectrin is present in *sphᴶ/sphᴶ* and *sph²ᴮᶜ/sph²ᴮᶜ* but not in *sph/sph* (Figure 3C).

### RBC deformability

The instability of *sph²ᴮᶜ/sph²ᴮᶜ* and *sphᴶ/sphᴶ* red blood cells is predicted by their severe microcytic anemia (RBC counts and hematocrits levels are less than 50% of normal) and extremely high levels of compensatory reticulocytosis (90%-95%).[2] Heterozygous mice are phenotypically and hematologically normal. Osmotic deformability profiles of blood samples from wild-type (+/+), heterozygous (*sph²ᴮᶜ/+* and *sphᴶ/+*), and homozygous

**Figure 2. Mutation in sphᴶ.** (A) Top, schematic representation of the *Spna1* cDNA with numbers above the line corresponding to the repeats of 106 aa that comprise the α-spectrin protein. Shown below the cDNA schematic are nucleotide (top) and amino acid (bottom) sequence of the +/+ and *sphᴶ/sphᴶ* cDNAs. (B) Genomic PCR of tail DNA from +/+ and *sphᴶ/+* mice. Lane M is marker; sizes in kb are shown on left. Lanes labeled 50: PCR products from a reaction containing primers (47 and 50) that amplify wild-type and mutant alleles of *Spna1*. Lanes labeled 50 and 49: PCR products from a reaction containing primers (47 and 49) designed to identify the C→A transition in the *sphᴶ* allele. Genotypes of mice are noted above each bracketed pair of reactions.

Figure 3. Downstream effects of mutations. (A) Northern blots of total RNA from spleen (lanes 1-3) and reticulocytes (lanes 4-6) of +/+ (lanes 1,4), $sph^J/sph^J$ (lanes 2,5), and $sph^{2BC}/sph^{2BC}$ (lanes 3,6) mice. UV shadowing was used to check RNA loading. (B) Laemmli SDS-PAGE of RBC ghost proteins from +/+ (lane 4) and mutant (lanes 1-3) mice. Genotype of mice is indicated above each lane. Size markers are indicated on the left; relative positions of $\alpha$-spectrin ($\alpha$) ankyrin (ANK), $\beta$-spectrin ($\beta$), and band 3 (b3) are indicated on the right. Ratios of $\alpha$, ANK, and $\beta$ to b3 are provided in Table 1. (C) Immunoblot of RBC ghost proteins from +/+ (lane 4) and mutant (lanes 1-3) mice. Genotype of mice is indicated above each lane. Primary antibody (1:250 dilution) detects $\alpha$ and $\beta$ spectrin equally. Size markers are indicated on the left; relative positions of $\alpha$ and $\beta$ spectrin are indicated on the right.

($sph^{2BC}/sph^{2BC}$ and $sph^J/sph^J$) mice are shown in Figure 4. The maximum value of the deformability index attained at physiologically relevant osmolality ($DI_{max}$) is quantitatively related to the mean surface area of the cells.[29] The osmolality at which the deformability index reaches a minimum in the hypotonic region of the gradient ($O_{min}$) is a measure of the osmotic fragility of the cells. RBCs from heterozygotes do not have significantly different osmotic deformability profiles than wild-type RBCs. In contrast, RBCs from $sph^{2BC}/sph^{2BC}$ and $sph^J/sph^J$ mice exhibit a profound decrease in surface area (decreased $DI_{max}$) and a marked increase in osmotic fragility (increased $O_{min}$). The decrease in surface area is consistent with the marked fragmentation of the mutant RBCs seen on peripheral blood smears.[32]

**Table 1. Ratios of $\alpha$-spectrin, ankyrin, and $\beta$-spectrin in normal and mutant mice**

| Genotype | $\alpha$:b3 | ANK:b3 | $\beta$:b3 |
|---|---|---|---|
| WBB6F1-$sph/sph$ | 0 | 1.3 | 1.2 |
| WBB6F1-$sph^{2BC}/sph^{2BC}$ | 0 | 1.6 | 1.6 |
| WBB6F1-$sph^J/sph^J$ | 1.7 | 2.0 | 2.8 |
| WBB6F1-+/+ | 22.0 | 7.9 | 20.0 |

Values represent densitometry of $\alpha$-spectrin ($\alpha$), $\beta$-spectrin ($\beta$), ankyrin (ANK), and band 3 (b3) on SDS-PAGE (Figure 3B).
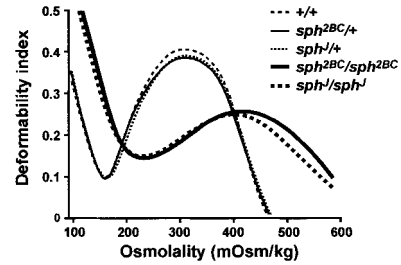


Figure 4. Osmotic deformability profiles of RBCs from wild-type (+/+), heterozygous ($sph^{2BC}/+$ and $sph^J/+$), and homozygous ($sph^{2BC}/sph^{2BC}$ and $sph^J/sph^J$) mice.

## Membrane attachment of $sph^J/sph^J$ spectrin

Previously, we showed that reticulocytes from $sph^J/sph^J$ mice synthesize de novo 1.5 times more $\beta$-spectrin and 6 times more $\alpha$-spectrin than reticulocytes from normal mice. In addition, the newly synthesized $\alpha$-spectrin is incorporated into the $sph^J/sph^J$ membrane at a 6-fold higher rate than normal.[30] Despite these observations, only 20% of the normal amount of $\alpha$-spectrin is present in mature $sph^J/sph^J$ erythrocyte ghosts at steady state. One possible explanation for this is that $sph^J$ spectrin binds to the membrane skeleton, but the binding is unstable, thereby allowing more rapid turnover of the bound mutant spectrin.

To investigate the possibility that $sph^J$ $\alpha$-spectrin forms a less stable link to the membrane skeleton than normal $\alpha$-spectrin, a double-label experiment was performed. The experiment was designed to allow [35S]-labeled $\alpha$-spectrin to enter the soluble $\alpha$-spectrin pool 30 minutes before the entry of [3H] $\alpha$-spectrin, allowing us to monitor the displacement of bound [35S]-labeled $\alpha$-spectrin by [3H]-labeled $\alpha$-spectrin. Normal and $sph^J/sph^J$ reticulocytes were incubated as follows: 15 minutes with [35S] methionine, 15 minutes with 5 mg/mL cold methionine, 15 minutes with [3H] leucine, and 120 minutes with cold methionine and leucine, 5 mg/mL each. Two washes in basic media were performed between each step.

The ratio of [3H]-to-[35S]–labeled $\alpha$-spectrin in the membrane skeleton of +/+ and $sph^J/sph^J$ reticulocytes at various times during the 120 minutes chase are shown in Figure 5. Data for each time point are the average of 3 experiments and, by being presented as ratios, are internally normalized. It is important to note that the ratio of [3H]/[35S] in the total spectrin pool was the same (0.47) for each genotype at the beginning and at the end of the 120-minute chase. The fact that this ratio remained stable throughout the course of the chase indicates that the $\alpha$-spectrin pool is relatively stable. As can be seen from the graph, the time required to reach half-equilibrium levels ([3H]/[35S] = 0.41) is 2.3 times faster in
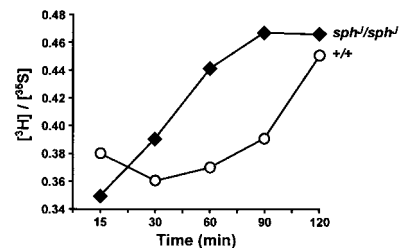


Figure 5. Binding of $\alpha$-spectrin to $sph^J/sph^J$ and +/+ reticulocyte membranes. Reticulocyte cultures from each were exposed sequentially for 15-minute intervals to [35S] methionine, unlabeled methionine, and [3H] leucine. During a 2-hour chase in unlabeled methionine and leucine, samples were removed, ghosts made, and the [3H]/[35S] ratios determined from gel-purified $\alpha$-spectrin. Ratios presented are the averages of 3 experiments ($P < .01$).

$sph^J/sph^J$ than in $+/+$ cells, suggesting a more rapid turnover of the newly synthesized mutant α-spectrin compared with normal. This result is consistent with the $sph^J$ α-spectrin skeleton link being less stable than normal.

## Discussion

Three major conclusions can be drawn from this study. First, the $sph^{2BC}$ and $sph^J$ mutations in Spna1 are molecularly and functionally distinct from each other and from a third severe HS-producing Spna1 mutation, sph, and from the HE-producing Spna1 mutation, $sph^{Dem}$. Second, the splice site mutation in intron 41 of $sph^{2BC}$ is responsible for exon skipping, premature termination, barely detectable protein, and membrane instability of the red cells. Third, the nonsense mutation in $sph^J$ that eliminates the C-terminal 0.5% of the protein leads to increased osmotic fragility as a result of the loss of cytoskeleton stability.

The $sph^{2BC}$ mutation is similar to the mutation $sph^{Dem}$ in causing exon skipping in the mRNA, but the effects of the exon skip in the 2 mutants are different. In $sph^{Dem}$, the exon skip does not shift the reading frame, and it produces a mutant protein fully capable of incorporation into the cytoskeleton but defective in tetramerization.[16] In $sph^{2BC}$, the exon skip introduces a frame-shift and premature termination, resulting in a truncated protein lacking sequences required for dimerization with β-spectrin and incorporation into the membrane; this truncated protein is likely rapidly degraded.[33] The presence of the premature stop codon in $sph^{2BC}$ mRNA may activate the nonsense-mediated mRNA decay pathway, leading to rapid turnover of the mutant mRNA.[34-36] In this respect, $sph^{2BC}$ more closely resembles the sph mutation, a single base deletion that also leads to premature protein termination and rapid mRNA degradation.[4]

The location of the $sph^{2BC}$ mutation in murine α-spectrin is comparable to that of the HE-associated LELY mutations of human α-spectrin, a set of 3 linked mutations in exon 40, intron 45, and intron 46.[37,38] The intron 45 mutation of $αL^{ELY}$ also produces exon skipping,[37] as do other mutations located farther 5′ in human α-spectrin, including the HE alleles $α^{Dayton}$, $α^{Oran}$, and $α^{St. Claude}$, and the HS allele $α^{Prague}$.[39-42]

In contrast to the effects of the $sph^{2BC}$ mutation, the $sph^J$ mutation does not eliminate the dimerization site of α-spectrin.[33] In fact, dimerization and tetramerization of the $sph^J$ α-spectrin protein can occur, as evidenced by the steady state levels of cytoskeletal proteins prepared from equivalent numbers of $+/+$ and mutant reticulocytes (Figure 3B) and by a previous study documenting normal dimer-tetramer ratios in $sph^J/sph^J$ ghosts.[16] Despite these findings, $sph^J/sph^J$ α-spectrin is unstable in the membrane-bound cytoskeleton (Figure 5 and Bodine et al[2]). The rapid uptake of the radiolabeled protein indicates sites are continuously made available for membrane binding. This would occur if the protein were degraded in situ or were unstably bound. Although we cannot distinguish between these alternatives conclusively, the equivalence of radioisotope in the total spectrin pool at 0 and at 120 minutes after incubation suggests that the pool of α-spectrin remains relatively steady. The more rapid increase of the $[^3H]/[^{35}S]$ ratio in $sph^J/sph^J$ vs $+/+$ α-spectrin in the membrane is consistent with a less stable membrane α-spectrin linkage in the mutant. Regardless of the interpretation, the COOH-terminal 13 aa of α-spectrin appear to be critical to its stability in the membrane skeleton because the mature erythrocyte ghosts of $sph^J/sph^J$ animals contain only 20% of the normal α-spectrin complement.

Structural features of the missing 13 aa suggest ways in which they may contribute to the stability of α-spectrin in the membrane. Four of these 13 aa are potential sites for phosphorylation (2 tyrosines, 1 serine, 1 threonine), and their loss may destabilize binding. To date, only phosphorylation of β-spectrin has been documented in intact RBCs.[43]

The 13 C-terminal residues are separated from the EF hand motifs of α-spectrin[33] by 60 aa; we believe this makes it unlikely that the deletion of these residues in the $sph^J$ protein affects the function of the EF hands. The deleted residues are within the segment of the spectrin tetramer involved in junctional complex (JC) formation.[44] To date, studies of interactions of spectrin with JC proteins such as protein 4.1, adducin, and F-actin have identified contact points on β-spectrin but not α-spectrin.[44-47] However, several analyses of the spectrin/protein 4.1/actin interaction[48-50] have indicated that isolated α- and β-spectrin chains interact with protein 4.1, protein 4.1–mediated binding of spectrin to actin requires the presence of both subunits of spectrin, and the region of β-spectrin that binds actin and protein 4.1 is closely associated with the carboxy terminus of α-spectrin. It is possible the 13 aa deleted in $sph^J$ represent a heretofore undiscovered binding site in α-spectrin for JC proteins. Based on the current knowledge of spectrin/JC interactions, we believe it is more likely that this region of α-spectrin is critical in stabilizing the configuration of β-spectrin to promote its binding to JC proteins. Without the interaction with the JC, the spectrin tetramer is tethered to the membrane solely through its ankyrin contacts, which may be insufficient in $sph^J/sph^J$ for spectrin and overall cytoskeleton stability. Further analyses of the $sph^J$ α-spectrin protein and of the 13 deleted amino acids could yield insight into the role of α-spectrin in JC formation and the mechanism through which spectrin stability is disrupted in $sph^J/sph^J$ mice.

## Acknowledgments

## References

1. Greenquist AC, Shohet SB, Bernstein SE. Marked reduction of spectrin in hereditary spherocytosis in the common house mouse. Blood. 1978;51:1149-1155.

2. Bodine DM IV, Birkenmeier CS, Barker JE. Spectrin-deficient inherited hemolytic anemias in the mouse: characterization by spectrin synthesis and mRNA activity in reticulocytes. Cell. 1984;37: 721-729.

3. Birkenmeier CS, McFarland-Starr EC, Barker JE. Chromosomal location of three spectrin genes: relationship to the inherited hemolytic anemias of mouse and man. Proc Natl Acad Sci U S A. 1988; 85:8121-8125.

4. Wandersee NJ, Birkenmeier CS, Gifford EJ, Mohandas N, Barker JE. Murine hereditary spherocytosis, sph/sph, is caused by a mutation in the erythroid α-spectrin gene. Hematol J. 2000;1:235-242.

5. Bloom ML, Birkenmeier CS, Barker JE. Complete nucleotide sequence of the murine erythroid β-spectrin cDNA and tissue-specific expression in normal and jaundiced mice. Blood. 1993;82: 2906-2914.

6. White RA, Birkenmeier CS, Peters LL, Barker JE, Lux SE. Murine erythrocyte ankyrin cDNA: highly conserved regions of the regulatory domain. Mamm Genome. 1992;3:281-285.

7. Winkelmann JC, Leto TL, Watkins PC, et al. Molecular cloning of the cDNA for human erythrocyte α-spectrin. Blood. 1988;72:328-334.

8. Winkelmann JC, Chang JG, Tse WT, Scarpa AL, Marchesi VT, Forget BG. Full-length sequence of

the cDNA for human erythroid beta-spectrin. J Biol Chem. 1990;265:11827-11832.

9. Lux SE, John KM, Bennett V. Analysis of cDNA for human erythrocyte ankyrin indicates a repeated structure with homology to tissue-differentiation and cell-cycle control proteins. Nature. 1990;344:36-42.

10. Lambert S, Yu H, Prchal JT, et al. cDNA sequence for human erythrocyte ankyrin. Proc Natl Acad Sci U S A. 1990;87:1730-1734.

11. Kam Z, Josephs R, Eisenberg H, Gratzer WB. Structural study of spectrin from human erythrocyte membranes. Biochemistry. 1977;16:5568-5572.

12. Tse WT, Lux SE. Red blood cell membrane disorders. Br J Haematol. 1999;104:2-13.

13. Bloom ML, Kaysser TM, Birkenmeier CS, Barker JE. The murine mutation jaundiced is caused by replacement of an arginine with a stop codon in the mRNA encoding the ninth repeat of β-spectrin. Proc Natl Acad Sci U S A. 1994;91:10099-10103.

14. Birkenmeier CS, Gifford EJ, Barker JE. The murine hereditary spherocytosis mutation, normoblastosis, is caused by a single base deletion in the erythroid ankyrin gene and produces a partially functional truncated ankyrin [abstract]. Blood. 2000;96:594.

15. Yi SJ, Liu SC, Derick LH, et al. Red cell membranes of ankyrin-deficient *nb/nb* mice lack band 3 tetramers but contain normal membrane skeletons. Biochemistry. 1997;36:9596-9604.

16. Wandersee NJ, Roesch AN, Hamblen NR, et al. Defective spectrin integrity and neonatal thrombosis in the first mouse model for severe hereditary elliptocytosis. Blood. 2001;97:543-550.

17. Kaysser TM, Wandersee NJ, Bronson RT, Barker JE. Thrombosis and secondary hemochromatosis play major roles in the pathogenesis of jaundiced and spherocytic mice, murine models for hereditary spherocytosis. Blood. 1997;90:4610-4619.

18. Bernstein SE. Inherited hemolytic anemia in mice: a review and update. Lab Anim Sci. 1980;30:197-205.

19. Barker JE, Kaysser-Kranich TM, Hamblen N, Deveau S. Multiple high cell dose injections of normal marrow into newborn jaundiced mice dramatically prolong life despite transient repopulation. Exp Hematol. 1999;27:966-971.

20. Wandersee NJ, Lee JC, Deveau SA, Barker JE. Reduced incidence of thrombosis in mice with hereditary spherocytosis following neonatal treatment with normal hematopoietic cells. Blood. 2001;97:3972-3975.

21. Wandersee NJ, Tait JF, Barker JE. Erythroid phosphatidyl serine exposure is not predictive of thrombotic risk in mice with hemolytic anemia. Blood Cells Mol Dis. 2001;29:75-83.

22. Chui DHK, Patterson M, Bayley ST. Unequal α

and β globin mRNA in reticulocytes of normal and mutant (*f/f*) fetal mice. Br J Haematol. 1980;44:431-439.

23. Sanger F, Nicklen S, Coulson AR. DNA sequencing with chain-terminating inhibitors. Proc Natl Acad Sci U S A. 1977;74:5463-5467.

24. Perkin-Elmer Cetus Corporation. Rapid, efficient DNA extraction for PCR from cells or blood. Amplifications. 1989;2:1-3.

25. Thurston SJ, Saffer JD. Ultraviolet shadowing nucleic acids on nylon membranes. Anal Biochem. 1989;178:41-42.

26. Laemmli UK. Cleavage of structural proteins during the assembly of the head of bacteriophage T4. Nature. 1970;227:680-685.

27. Fairbanks G, Steck TL, Wallach DFH. Electrophoretic analysis of the major polypeptides of the human erythrocyte membrane. Biochemistry. 1971;10:2606-2616.

28. White RA, Birkenmeier CS, Lux SE, Barker JE. Ankyrin and the hemolytic anemia mutation, *nb*, map to mouse chromosome 8: presence of the *nb* allele is associated with a truncated erythrocyte ankyrin. Proc Natl Acad Sci U S A. 1990;87:3117-3121.

29. Clark MR, Mohandas N, Shohet SB. Osmotic gradient ektacytometry: comprehensive characterization of red cell volume and surface maintenance. Blood. 1983;61:899-910.

30. Barker JE, Bodine DM, Birkenmeier CS. Synthesis of spectrin and its assembly into the red blood cell cytoskeleton of normal and mutant mice. In: Bennett V, Lux SE, Cohen CM, Palek J, eds. Membrane skeletons and cytoskeletal-membrane associations. New York, NY: Alan J Liss; 1986:313-324.

31. Sidman C. Two-dimensional electrophoresis. Immunol Methods. 1981;2:57-74.

32. Bernstein SE. Hereditary disorders of the rodent erythron: genetics in laboratory animal medicine. Natl Acad Sci Publ. 1969;1679:9-33.

33. Speicher DW, Weglarz L, DeSilva TM. Properties of human red cell spectrin heterodimer (side-to-side) assembly and identification of an essential nucleation site. J Biol Chem. 1992;267:14775-14782.

34. Whitfield TT, Sharpe CR, Wylie CC. Nonsense-mediated mRNA decay in *Xenopus* oocytes and embryos. Dev Biol. 1994;165:731-734.

35. Liu HX, Cartegni L, Zhang MQ, Krainer AR. A mechanism for exon skipping caused by nonsense or missense mutations in *BRCA1* and other genes. Nat Genet. 2001;27:55-58.

36. Neu-Yilik G, Gehring NH, Thermann R, Frede U, Hentze MW, Kulozik AE. Splicing and 3′ end formation in the definition of nonsense-mediated decay-competent human beta-globin mRNPs. EMBO J. 2001;20:532-540.

37. Wilmotte R, Marechal J, Morle L, et al. Low ex-

pression allele αL$^{ELY}$ of red cell spectrin is associated with mutations in exon 40 (α$^{V/41}$ polymorphism) and intron 45 and with partial skipping of exon 46. J Clin Invest. 1993;91:2091-2096.

38. Wilmotte R, Marechal J, Delaunay J. Mutation at position of −12 of intron 45 (c→t) plays a prevalent role in the partial skipping of exon 46 from the transcript of allele αL$^{ELY}$ in erythroid cells. Br J Haematol. 1999;104:855-859.

39. Hassoun H, Coetzer TL, Vassiliadis JN, et al. A novel mobile element inserted in the α-spectrin gene: spectrin Dayton, a truncated α-spectrin associated with hereditary elliptocytosis. J Clin Invest. 1994;94:643-648.

40. Alloisio NR, Wilmotte J, Marechal P, et al. A splice site mutation of α-spectrin gene causing skipping of exon 18 in hereditary elliptocytosis. Blood. 1993;81:2791-2798.

41. Fournier CM, Nicolas G, Gallagher PG, Dhermy D, Grandchamp B, Lecomte M-C. Spectrin St. Claude, a splicing mutation of the human α-spectrin gene associated with severe poikilocytic anemia. Blood. 1997;89:4584-4590.

42. Wichterle H, Hanspal M, Palek J, Jarolim P. Combination of two mutant alpha spectrin alleles underlies a severe spherocytic hemolytic anemia. J Clin Invest. 1996;98:2300-2307.

43. Harris HW Jr, Lux SE. Structural characterization of the phosphorylation sites of human erythrocyte spectrin. J Biol Chem. 1980;255:11512-11520.

44. Bennett V. The spectrin-actin junction of erythrocyte membrane skeletons. Biochim Biophys Acta. 1989;988:107-121.

45. Mische SM, Mooseker MS, Morrow JS. Erythrocyte adducin: a calmodulin-regulated actin-bundling protein that stimulates spectrin-actin binding. J Cell Biol. 1987;105:2837-2845.

46. Sears DE, Marchesi VT, Morrow JS. A calmodulin and alpha-subunit binding domain in human erythrocyte spectrin. Biochim Biophys Acta. 1986;870:432-442.

47. Cohen CM, Foley SR. Biochemical characterization of complex formation by human erythrocyte spectrin, protein 4.1, and actin. Biochemistry. 1984;23:6091-6098.

48. Cohen CM, Langley RJ. Functional characterization of human erythrocyte spectrin alpha and beta chains: association with actin and erythrocyte protein 4.1. Biochemistry. 1984;23:4488-4495.

49. Coleman TR, Harris AS, Mische SM, Mooseker MS, Morrow JS. Beta spectrin bestows protein 4.1 sensitivity on spectrin-actin interactions. J Cell Biol. 1987;104:519-526.

50. Becker PS, Schwartz MA, Morrow JS, Lux SE. Radiolabel-transfer cross-linking demonstrates that protein 4.1 binds to the N-terminal region of β spectrin and to actin in binary interactions. Eur J Biochem. 1990;193:827-836.